ME - 259 Finite Element Analysis Project

Heat Transfer Analysis on Sample Holder for Porous Materials

Colin Hodge & Dan Jordan

December 11, 2020

Contents

1 Project Overview

The aerospace industry is one that is always evolving, as more is constantly being discovered on how to make frequent space and upper travel atmospheric not only safer, but more accessible. Although getting into the upper atmosphere is a huge feat on its own, traveling in it and returning safely is another. Upon reentry into Earth's lower atmosphere there are extreme thermal loads present, which requires some form of heat shield to be present on the reentry vehicle in order to protect any payloads or human occupants that may be inside. Typically, an ablative or extremely heat resistant material to be used on the outside of the reentry vehicle to allow for almost perfect insulation of the cabin. This ablative material was mainly used on the leading edge of the vehicle, which is the component that undergoes the most intense thermal loads in the entire system.

For years, the solution to intense thermal loads on upper atmospheric travel was to round the leading edges so they would be blunt enough to stop the heat from damaging the system. A commonly used material was a ceramic known as reaction cooled glass. Although effective as a heat shield, this material could not withstand any water, which limited the days air crafts could be flown. Even though it had flaws, it was an industry standard for many upper atmospheric traveling vehicles, more specifically on NASA's X-43 Scramjet (Figure 1). Testing materials for heat shielding capabilities during this reentry phase is too expensive and risky to even attempt, so facilities have been constructed to recreate these conditions as accurately as possible for testing purposes. One such facility is the University of Vermont's Inductively Coupled Plasma Torch Facility.

Figure 1: NASA's X-43 Scramjet

The UVM Inductively Coupled Plasma Torch (ICP Torch) facility located in the Discovery Science building is used to recreate the upper atmospheric conditions experienced in reentry. Most recently, the lab has been studying materials that will be used for the leading edges of these reentry vehicles. The leading edge is the location of the vehicle that will experience the highest thermal loads upon reentry into the atmosphere. A new porous material has been designed and manufactured for use on the leading edge (Figure 2). The idea is that an injection gas will be pumped into the porous material and exit through the pores, thus creating a layer of gas around the material and the leading edge of the vehicle. However, due to its novelty, there is not a holder that exists to hold the sample porous material in place and monitor the conditions around it during testing in the UVM ICP torch facility.

Figure 2: The New Porous Sample to be Tested in the ICP Torch

In order to create something to effectively test this new permeable material, existing sample holder designs must be modified to be able to monitor the pressure conditions during testing and to allow for a transpiration gas to flow through the holder and into the sample. The constructed sample holder will attach to an existing probe in the ICP Torch facility known as the "Insertion Probe", this can be seen at work in the figure below denoted by the red arrow (Figure 3). The flow of the injection gas must also be monitored to learn how its cooling effects will help to mitigate the temperature at the leading edge. With the creation of a holder for the sample material, testing will be possible and progress will be made for developing an understanding for how this material can be used to make space travel more effective and safe.

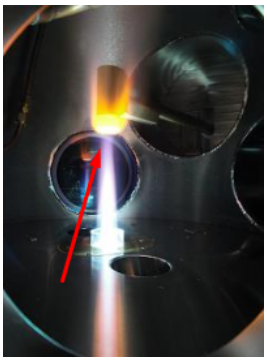

Figure 3: Insertion Probe During Testing (red arrow indicates where the sample holder will attach)

2 Theory

To conduct a FEA heat transfer study, the heat equation must first be understood. This can be done by looking at an infinitely small element, dx, in which heat is being conducted through the body by a stationary heat source, Q. Heat is transferred in one dimension, along the x-direction, and temperature can be assumed constant through any given cross section.

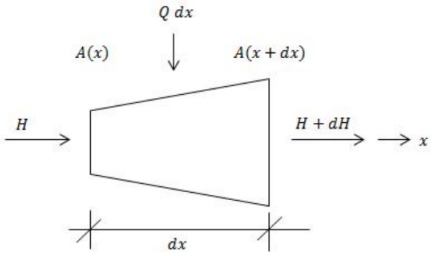

Figure 4: 1D infinitely small heat transfer element[8]

This derivation begins with steady state assumptions (i.e. no time dependency), however transient effects will also be looked into. According to the Conservation of Energy Law (Equation 1), the amount of heat energy H entering a body must be equal to the amount leaving it.

$$H + Qdx = H + dH \tag{1}$$

When simplified, heat transfer is seen as:

$$Q = \frac{dH}{dx} \tag{2}$$

In Equation 2, Q is heat transfer, $\frac{dH}{dx}$ is the change in heat with respect to a change in position. This can be further simplified after defining the equation for heat (Equation 3), where A is the cross sectional area, and q is heat flux.

$$H(x) = A(x)\, q(x) \tag{3}$$

After combining (2) and (3), heat transfer can be re-written as:

$$Q = \frac{d}{dx}(Aq) \tag{4}$$

Further expansion of the heat transfer equation, requires the equation for heat flux, which is given by Fourier's Law of Heat Conduction, where $u(x)$ represents temperature.

$$q = -k\frac{\delta u}{\delta x} \tag{5}$$

In Equation 5, k is thermal conductivity, and $\frac{\delta u}{\delta x}$ can be seen as the rate of change of temperature with respect to position. Thermal conductivity is written as negative due to the fact the heat always transfers from hot to cold, and k can be seen as the transport coefficient for conductive heat transfer. To show transient heat transfer effects, heat must change with time. Equation 4 can be modified to add time, t, through the integration of density, ρ, specific heat capacity, c, and $\frac{\delta u}{\delta t}$, which represents the change in temperature with respect to time. Specific heat capacity is known to be the amount of energy needed to raise the temperature of an element by one degree. With the addition of temperature changing with time, heat transfer is now written as:

$$Q = \frac{\delta}{\delta x}(Aq) + \rho c \frac{\delta u}{\delta t} \tag{6}$$

Now, combing (5) with (6), the differential equation for one-dimensional heat transfer can be seen in Equation 7.

$$Q = \rho c \frac{\delta u}{\delta t} - \frac{\delta}{\delta x}\left(Ak\frac{\delta u}{\delta x}\right) \tag{7}$$

In addition to the general heat transfer equation, the simulation utilizes heat transfer equations for conduction, convection, and radiation because these are the specific processes in which the heat will be transferred. The equations for heat transfer in terms of conduction, convection, and radiation are as follows:

$$\frac{dQ_{cond}}{dt} = \frac{-kA\Delta T}{d} \tag{8}$$

$$\frac{dQ_{conv}}{dt} = h_c A \Delta T \tag{9}$$

$$\frac{dQ_{rad}}{dt} = \sigma A \Delta T \tag{10}$$

In Equations 8, 9, and 10, A is surface area, ΔT is change in temperature, k is thermal conductivity, t is time, d is thickness, h_c is heat transfer coefficient, and σ is the Stefan-Boltzmann constant. The previously presented equations (8, 9, and 10) are simplified versions of the finite element method (FEM) equations which would be used to computationally solve by hand.

3 ABAQUS Model

The objective of this analysis is an understanding of the heat transfer on the sample holder (Figure 5) during testing. This understanding will be used to determine the best material for the sample holder out of copper and brass. Copper and brass were chosen as the two working materials due to their high thermal

conductivity's and low specific heats. These results will also provide information regarding the necessity of water cooling in the design. The analysis was run in two steps on ABAQUS, the first being a steady state heating step and the second being a transient cooling step.

Below (Figure 5) clearly labels all of the working parts in the porous sample holder modeled in ABAQUS. In the center is the porous sample being tested in the ICP Torch facility, also seen in figure 2. Attached to either side are the molybdenum end pieces that will be pre-welded to the porous sample in order for it to have a secure and rigid connection so that it will not fall off during testing. At every intersection is a Swagelok fitting (either a 90 degree elbow or a tee bend), these are being used because of their ability to hold a secure connection under extreme loads like the ones seen in this torch facility. All the surrounding pipes are the ones that are being analyzed in this simulation, to determine which material will be used in the final design. And due to its ability to rotate and translate freely in the flow the sample holder will attach to an existing probe in the test chamber (Figure 3), at the top the ABAQUS model is where the connection will take place.

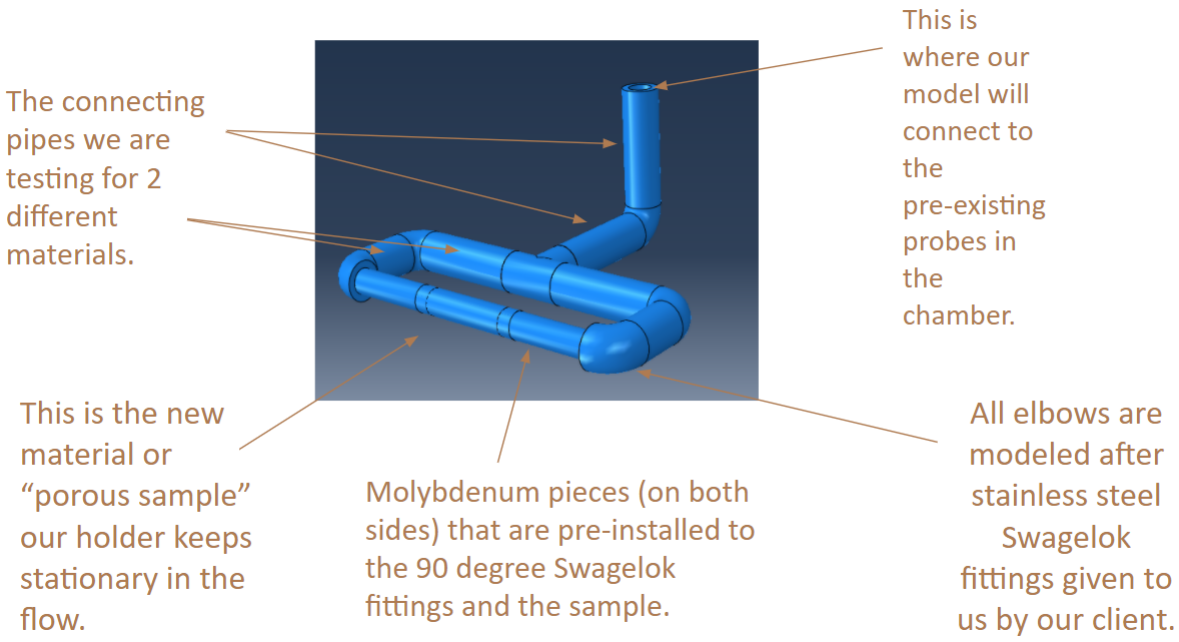

Figure 5: Labeled Sample Holder Modeled in ABAQUS Assembly

3.1 Material Properties

In order to conduct a heat transfer study in ABAQUS, properties of conductivity, specific heat, and density are necessary for each working material. The sample holder was designed in millimeters, so to keep consistency throughout the entire design units of millimeters, kilograms, and degrees Kelvin were used in this simulation. These working materials consist of the two being tested (Brass and copper), stainless steel for the Swagelok fittings, the molybdenum holding the sample in place, and the porous sample itself. The porous sample was designed and manufactured at the University of Colorado Boulder and its physical properties were received by that laboratory as they cannot be found anywhere else. Other material properties were found online and can be seen in the bibliography portion of the report [2–4] . Those material properties can be seen in the figures below (Figures 6, 7, 8, 9, 10).

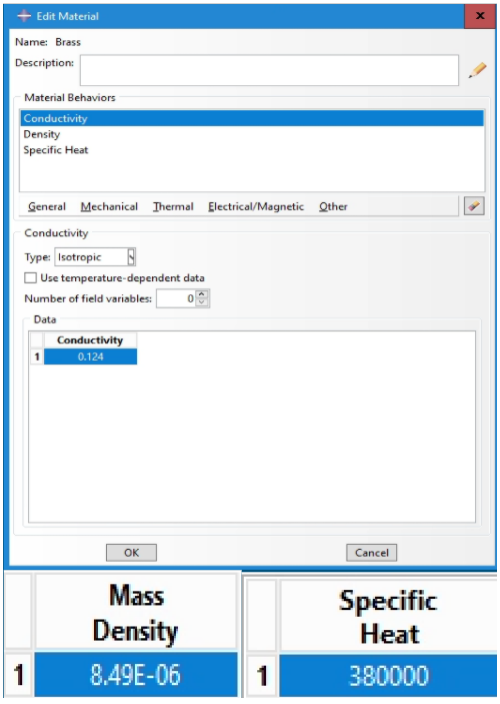

Figure 6: Material Properties of Brass

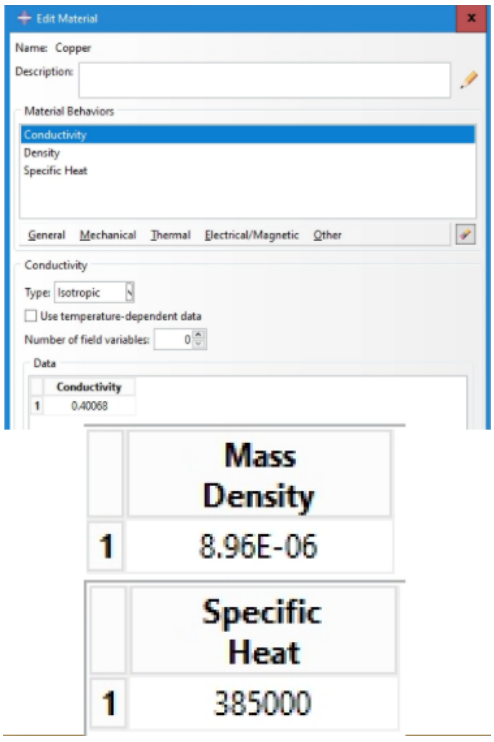

Figure 7: Material Properties of Copper

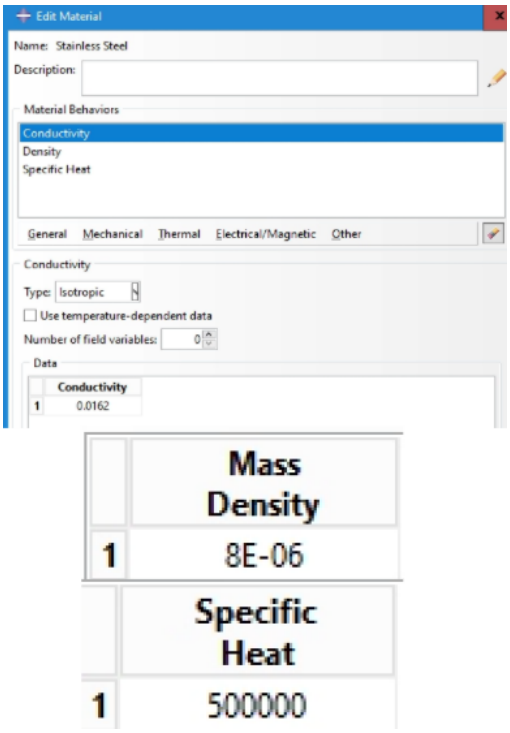

Figure 8: Material Properties of Stainless Steel

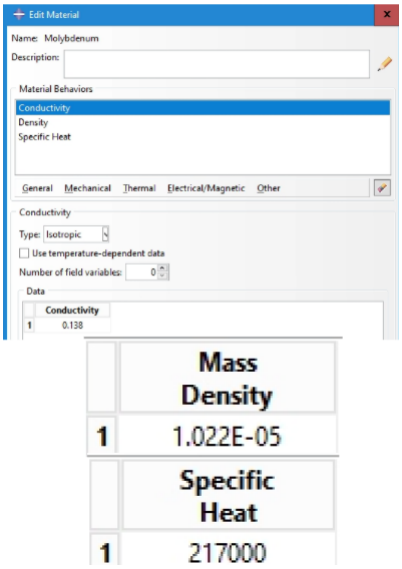

Figure 9: Material Properties of Molybdenum

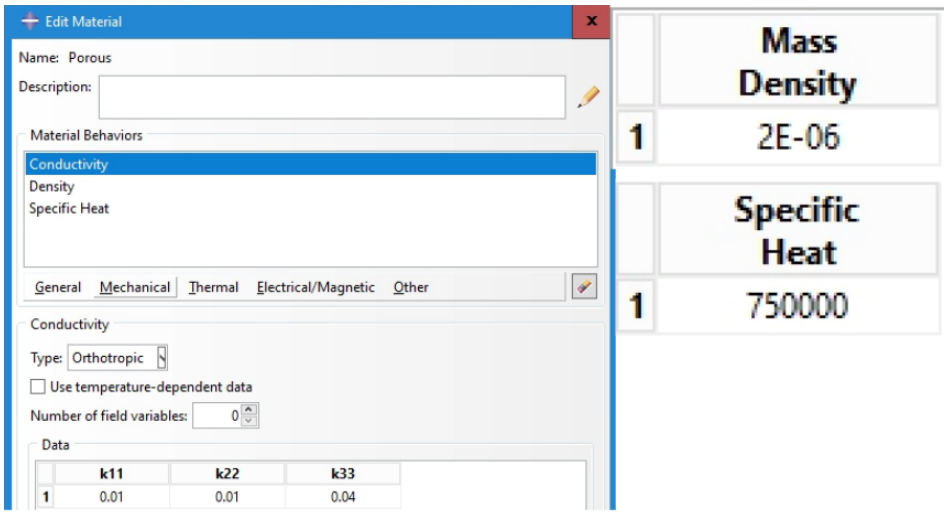

Figure 10: Material Properties of the Porous Sample

3.2 Boundary Conditions & Loads

To simulate the thermal loading provided by the ICP torch, a surface heat flux load of $3\frac{W}{mm^2}$ was placed on the surface of the porous material during heating. Upon full extension of the plasma torch, the torch only covers about two inches of the porous sample surface, thus the heat flux loading is modelled to cover two inches of the sample's surface, which can be seen as dimension L_2 in Figure 11.

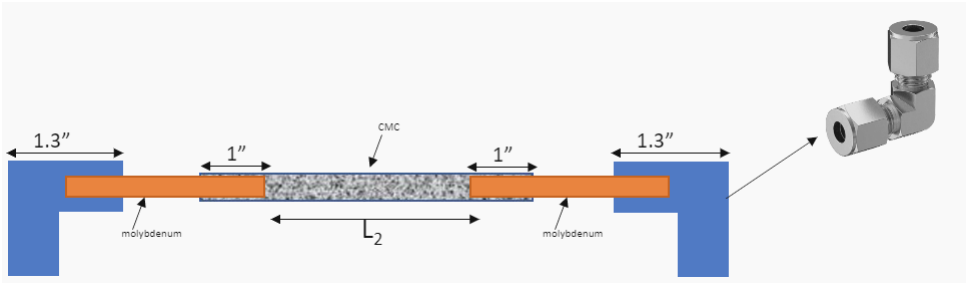

Figure 11: Front end of sample holder where the sample is attached.

A constant temperature boundary condition of 7000K is also placed on the sample surface. This is because the plasma will have a maximum temperature of about 7000K during testing, and will be constantly in contact with the sample surface. During cooling, the sample holder no longer has any loading provided

by the porous sample, or a constant temperature boundary condition.

3.3 Element Type & Meshing

Four out of the five parts (Molybdenum part, porous sample, insert from probe, and the right/left bend parts) in the modeled assembly are generally the same shape with some minor changes, seen in the figures below (Figures 12, 13, 14, & 15). Because of the similar geometry throughout (modeled after pipes and pipe fittings) the mesh style of those parts were completely identical. These parts were all modeled with a global seed size of 3.5 using a hexagonal mesh type. The element type was DC3D8 (An 8 node linear heat transfer brick), this element type, mesh type, and seed size allowed for fairly accurate results when the simulation was run, as the meshing of these parts was fairly easy and no issues came to the surface.

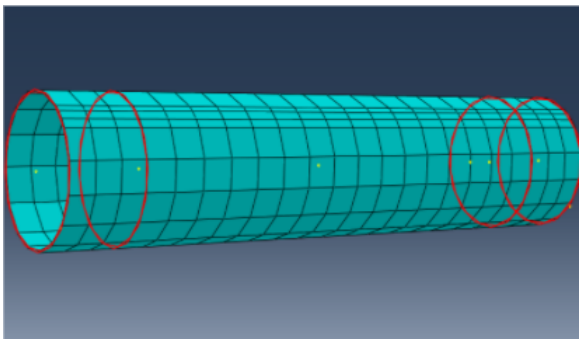

Figure 12: Meshed Porous Sample

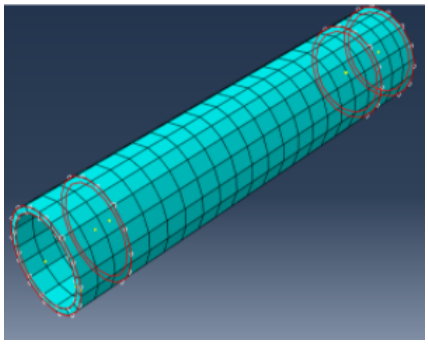

Figure 13: Meshed Molybdenum

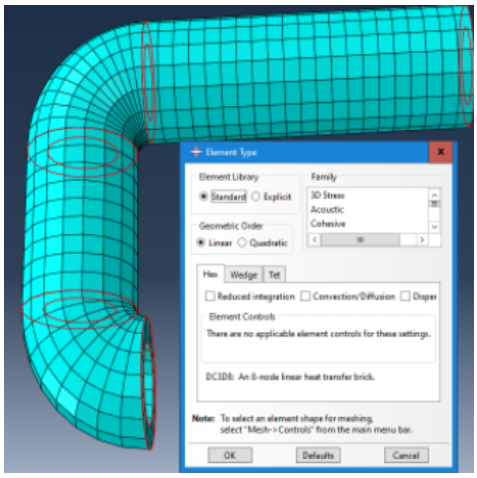

Figure 14: Meshed Right/Left Bend

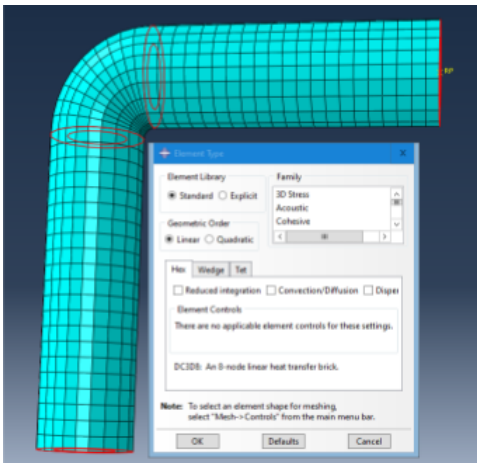

Figure 15: Meshed Insert From Probe

Unfortunately the remaining meshing of the parts did not go as easy as the previously discussed four parts. The "Tee bend" (Figure 16) holds a similar but relatively different geometry to the other parts, which led to some meshing problems with it. A global seed size of 3.5 was also applied to this part as well. Because of the multi-directional nature of the part it had some meshing errors and warnings when hexagonal mesh type was applied to it, these appeared around the corners of the tubing. These warnings led to meshing the part a with tetrahedral mesh type and was assigned a DC3D4 element type, known as a 4-node linear heat

transfer brick, this element type when compared to the other parts yielded less accurate results. The tee bend was not the main focus of the study and therefore the less accurate results was ruled not to be a huge issue when it came to the overall results of the simulation.

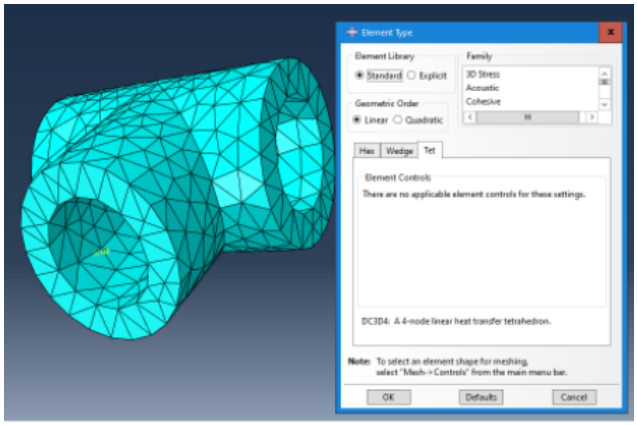

Figure 16: Meshed Tee Bend

4 Assumptions & Simplifications

The test chamber in which the sample and sample holder will be placed into for testing is seen in Figure 17. The ICP torch testing chamber operates as a vacuum, thus it is safe to assume that there would be no heat transfer due to convection during the heating step.

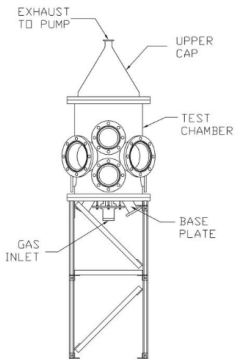

Figure 17: Scaled drawing of the ICP torch test chamber[1]

The ambient air near the torch during testing is is known to be between 400 and 500K, which decreases to around room temperature near the chamber walls. To simulate vacuum conditions and know ambient air conditions, only conduction and radiation interactions were input to ABAQUS during the heating step. To establish radiation interactions, emissivity values must be known for each material, along with the respective surrounding ambient temperatures. With a known range of air temperatures during the heating phase, the ambient temperatures for the front of the sample holder were placed at 500K, 450K at the mid-section, and 400K at the back of the sample holder where it would attach to the insertion probe. The ambient temperature locations in relation to the sample holder can be seen in Figure 18.

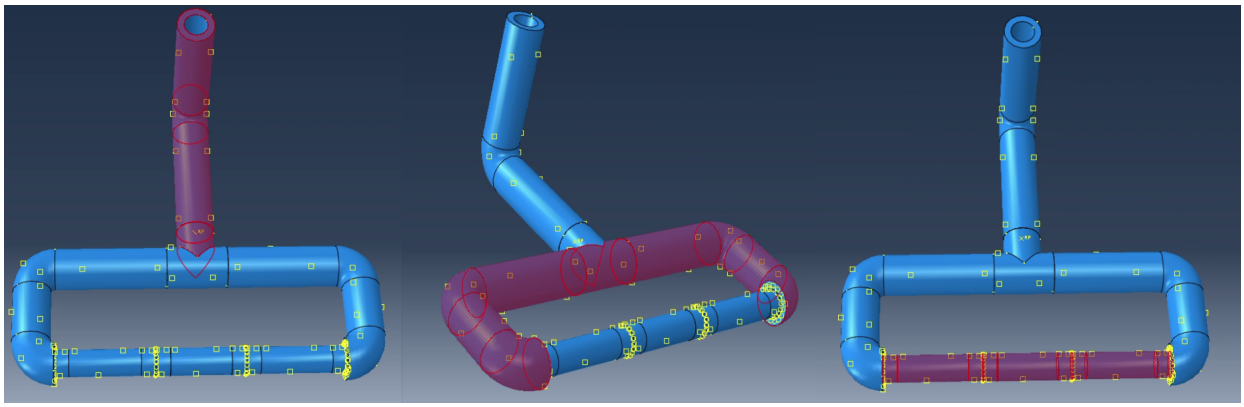

Figure 18: Air temperatures surrounding the sample holder from left to right: 400K, 450K, 500K.

A pre-defined temperature field of 293K was placed on all nodes of the sample holder before the heating step to indicate that the holder will be starting at room temperature. During cooling, the holder will be simulated as being outside the testing chamber at room temperature. Since the holder is no longer in a vacuum at this point, convective losses will be simulated, along with conductive losses during cooling. To establish convective interactions, surface film conditions were placed on all surfaces exposed to the air, where input of the free air heat transfer coefficient and temperature of the surrounding air was necessary. All interfacing parts of the sample holder are also assumed to have no thermal resistance during both steps. This simplification was made to make modelling of the ICP torch's testing conditions and sample holder interactions more attainable.

5 Results & Conclusion

5.1 Results

Temperature versus time graphs were obtained for both copper and brass during the heating and cooling steps. Results were taking from the portion of the sample holder seen in red in Figure 19.

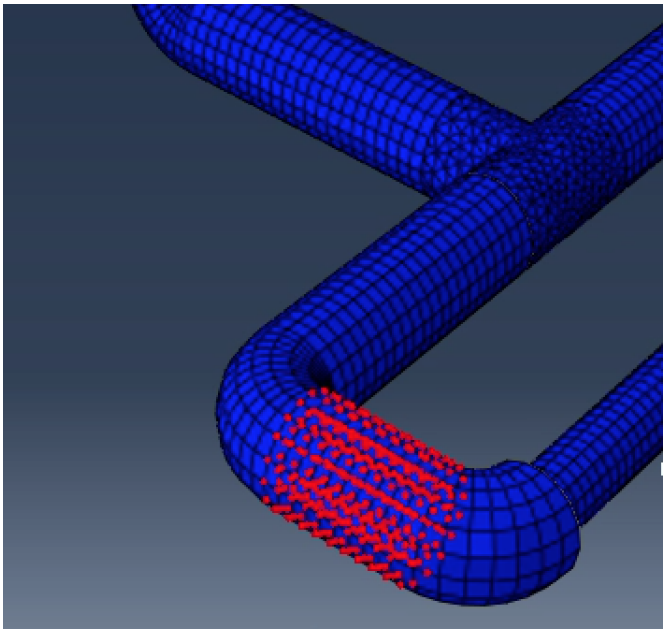

Figure 19: Portion of the sample holder being analyzed.

This portion of the sample holder was chosen to be analyzed because it is the section of material being tested that is closest to the plasma. The maximum temperature attained by the copper at this portion of the holder was 789.15K, while the maximum temperature of the brass was 775.87K. The temperature versus time graphs for the heat step of both materials can be seen in Figures 20 and 21.

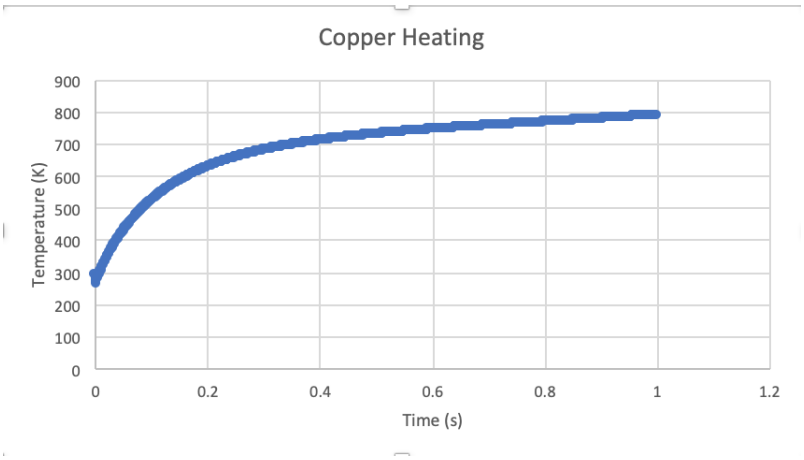

Figure 20: Copper heating step Temperature vs. Time graph

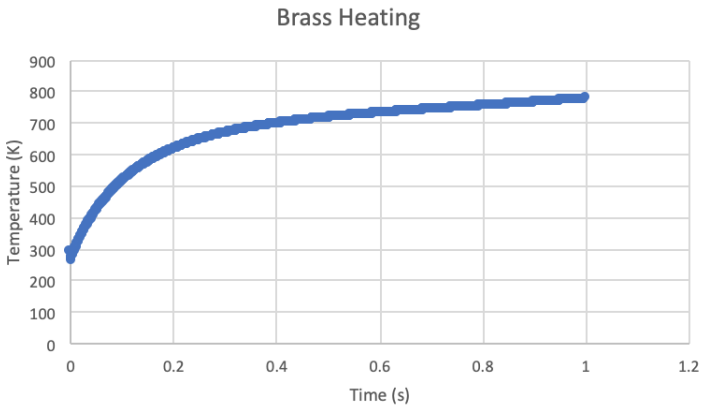

Figure 21: Brass heating step Temperature vs. Time graph

With both maximum temperatures being well below the respected melting points of the materials (1357.5K for copper and 1205.4K for brass), neither metal is at risk of failure. The temperature versus time graph for the cooling step of both materials can be seen in Figure 22.

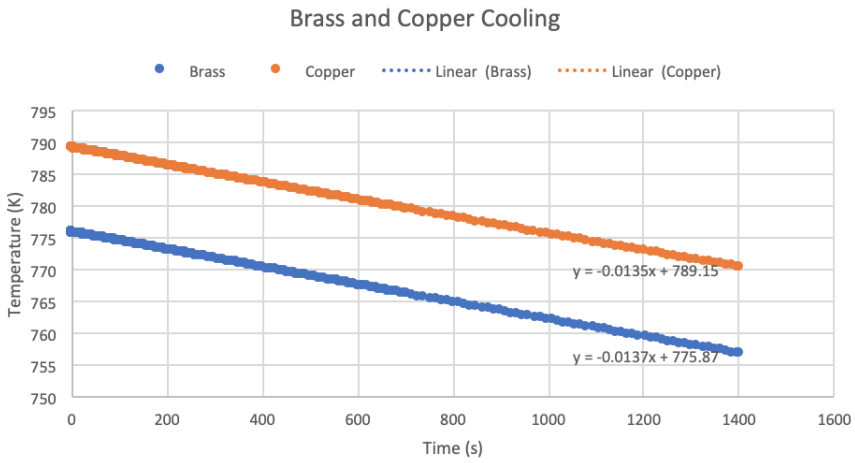

Figure 22: Brass and Copper cooling step Temperature vs. Time graph

The rate of cooling from both materials can be seen from the negative slope on the temperature vs. time graph in Figure 22. Copper had a cooling rate of -0.0135 K/s while brass had a cooling rate of -0.0137 K/s. With both materials reacting very similarly in terms of maximum temperature during heating, and cooling rates during the cooling, it can now be seen through results that either material would work well in the sample holder design. However, brass will be chosen as the working material.

5.2 Conclusion

Although cooling rates and temperature data are very similar between both materials, brass reached an overall lower temperature value than copper during maximum loading, and also maintained a slightly faster cooling rate. It is now known that both materials can withstand the thermal conditions provided by the plasma torch without failing, but it has not been determined if yield stressing will occur due to thermal expansion. Brass has a higher yield stress than copper, which will be important to consider with such high changes in temperature occurring during testing. If there were to have been noticeable differences in cooling rates between copper and brass, then the material with the faster cooling rate would have been chosen.

In terms of water cooling, it has been decided that this will no longer be necessary in the design due to the temperatures of both materials not reaching values close to failure. Additionally, the transpiration gas

that will be flowing through the internal piping to be injected to the porous sample was factored into the decision to not have water cooling. Although the main purpose of the transpiration gas is to study its heat shielding capabilities with the porous sample, it will also provide some cooling capabilities to the internal walls of the piping and holder. Prior to conducting this study, the client, Professor Douglas Fletcher, hinted that water cooling may not be necessary in the design due to the experimental conditions and presence of the transpiration gas. However, this study was conducted to confirm this theory and to see the capabilities of copper and brass in the design.

This ABAQUS model and simulation will be stored and referenced throughout the remainder of the senior design process. Improvements will also be made to the file to increase accuracy and refine results to the best possible degree. With the many simplifications and assumptions made to ensure the job would run successfully with somewhat accurate results, many improvements will be made for the future. Some of these improvements may include: decreasing the mesh size, making the heating step into a transient step, and the inclusion of transpiration gas flow in the model. As the model is built upon over time, the mesh size can be decreased significantly, along with the heating step being made to transient to enhance the accuracy of results. With minimal errors during job submissions and increased modeling accuracy of the various testing conditions present in the ICP torch lab, more time can be afforded to run larger simulations because the results will be known to be accurate. The transpiration gas flow should also be included in the model eventually. With the addition of the transpiration gas flow, maximum temperatures reached during testing will change, along with stressing in the piping due to thermal expansion (a thermal stressing simulation was also made for the SEED class). This will thus make the simulation more realistic and generate results that will be more similar to actual testing in lab.

6 References

[1] D. G. Fletcher, J. M. Meyers, and W. P. Owens, "Development of a 30 kW Inductively Coupled Plasma Torch for Advanced Aerospace Material Investigations," *The University of Vermont*, February 2012.

[2] Pure Copper Material Properties. (n.d.). Retrieved December 06, 2020, from http://www-ferp.ucsd.edu/LIB/PROPS/PANOS/cu.html

[3] The Online Materials Information Resource. (n.d.). Retrieved December 06, 2020, from http://www.matweb.com/search/datasheet.aspx?matguid=5edc39d3b0fd44efa9fdd90d049c3737

[4] Brass Material Properties Data Sheet. (n.d.). Retrieved December 06, 2020, from http://www.matweb.com/search/DataSheet. aspx?MatGUID=d3bd4617903543ada92f4c101c2a20e5

[5] Dunbar, Brian. (n.d.). X-43A Aircraft. Retrieved from https://www.nasa.gov/centers/armstrong /history/experimntal_aircraft/X-43A.html

[6] What is Von Mises Stress?: SimScale Finite Element Analysis. (2020, October 09). Retrieved December 05, 2020, from https://www.simscale.com/docs/simwiki/fea-finite-element-analysis/what-is-von-mises-stress/

[7] SS-2-UT-3. (n.d.). Retrieved December 06, 2020, from https://www.swagelok.com/en/catalog/Product /Detail?part=SS-2-UT-3

[8] Schiren, W. (2018, June 24). Finite Element Method for 1D Transient Convective Heat Transfer Problems (Rep.). Retrieved from http://www.diva-portal.org/smash/get/diva2:1223250/FULLTEXT01.pdf